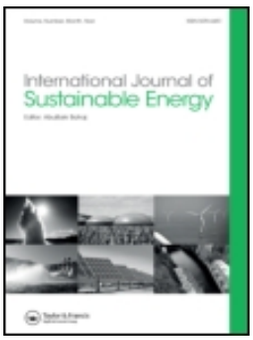

International Journal of Sustainable Energy

ISSN: 1478-6451 (Print) 1478-646X (Online) Journal homepage: http://www.tandfonline.com/loi/gsol20

Artificial breeding of an optimized solar tunnel dryer using genetic algorithms

Gareth M. Kituu , Douglas Shitanda , Chris Kanali , Joseph Mailutha & John Wainaina

To cite this article: Gareth M. Kituu , Douglas Shitanda , Chris Kanali , Joseph Mailutha & John Wainaina (2012) Artificial breeding of an optimized solar tunnel dryer using genetic algorithms, International Journal of Sustainable Energy, 31:5, 313-325, DOI: 10.1080/1478646X.2011.587010

To link to this article: https://doi.org/10.1080/1478646X.2011.587010

International Journal of Sustainable Energy
Vol. 31, No. 5, October 2012, 313–325

Taylor & Francis
Taylor & Francis Group

Artificial breeding of an optimized solar tunnel dryer using genetic algorithms

Gareth M. Kituu[a]*, Douglas Shitanda[b], Chris Kanali[b], Joseph Mailutha[b] and John Wainaina[c]

[a]*Department of Industrial, Manufacturing and Energy Engineering, South Eastern University College, P.O. Box 170-90200, Kitui, Kenya;* [b]*Biomechanical and Environmental Engineering Department, Jomo Kenyatta University of Agriculture and Technology, 62000-00200 Nairobi, Kenya;* [c]*Institute of Computer Science and Information Technology, Jomo Kenyatta University of Agriculture and Technology, 62000-00200 Nairobi, Kenya*

(*Received 4 January 2011; final version received 6 March 2011*)

Studies were carried out to artificially breed an optimized solar tunnel dryer using genetic algorithms (GAs). The energy harnessed by the dryer was simulated in Visual Basic Script (Microsoft Visual Basic Script 2010™) and the model was used to optimize the dryer by executing the Goal GA. The optimized dryer was developed and tested for energy harnessing against an existing solar tunnel dryer. The results of the analysis showed an 18–113% increase in plenum chamber temperature for the two dryers. Further, a two-way analysis of variance demonstrated the existence of a highly significant difference between plenum chamber temperatures for the two dryers ($F = 16.37$, $F_{\text{crit},0.99} = 2.89$). Furthermore, regression analysis and Student's t-test established the performance of the optimized dryer to be superior to that of the existing dryer. Finally, this study showed the effectiveness of Goal GA in artificial breeding of an optimized solar tunnel dryer.

Keywords: artificial breeding; genetic algorithm; solar tunnel dryer; optimization; simulation model; plenum chamber temperature

Nomenclature

A_b	Albedo of the surrounding area (m^2)
A_c	Collector plate surface area (m^2)
C_{pv}	Specific heat of humid air ($J\,kg^{-1}\,K^{-1}$)
F'	Collector efficiency factor (dimensionless)
H_{asl}	Altitude (m)
H_d	Daily diffuse solar radiation (MJ/m^2)
H_o	Extra-terrestrial solar energy incident on a horizontal surface (MJ/m^2)
H_g	Daily global solar radiation incident on a horizontal ground (MJ/m^2)
I_b	Direct solar radiation (W/m^2)
I_d	Diffuse radiation (W/m^2)

*Corresponding author. Email: mgm.kituu@yahoo.com

ISSN 1478-6451 print/ISSN 1478-646X online

http://dx.doi.org/10.1080/1478646X.2011.587010
http://www.tandfonline.com

I_c	Solar radiation absorbed by a collector plate per unit area per unit time (W/m^2)
I_g	Global solar radiation at a particular point on the ground (W/m^2)
k_t	Cloudiness ratio
$\dot{m}_a$	Mass flow rate of air (kg/s)
N	The numerical value of the day of the year
R_b	Tilt factor for beam radiation (dimensionless)
R_d	Tilt factor for diffuse radiation (dimensionless)
Rhop	Relative humidity (%) of plenum chamber air during testing of optimized solar tunnel dryer
Rhun	Relative humidity (%) of plenum chamber air during testing of existing solar tunnel
R_r	Tilt factor for reflected radiation (dimensionless)
S_a	Number of actual sunshine hours in a day
S_p	Number of possible sunshine hours in a day
T_i	Inlet air temperature (K)
T_i(op)	Inlet air temperature (°C) during testing of existing solar tunnel dryer
T_i(un)	Inlet air temperature (°C) during testing of existing solar tunnel dryer
T_p	Plenum chamber air temperature (K)
T_p(op)	Plenum chamber temperature (°C) for optimized solar tunnel dryer
T_p(un)	Plenum chamber temperature (°C) for existing solar tunnel dryer
U_L	Overall heat loss coefficient ($W\,m^{-2}\,K^{-1}$)
α	Absorptivity of the absorber plate ($W\,m^{-2}\,K^{-1}$)
δ	Angle of declination (degrees)
φ	Latitude (degrees)
τ	Transmissivity of the collector cover material (dimensionless)
ω_s	Sunset or sunrise hour angle (degrees)

1. Introduction

Despite the abundant availability of solar energy in the tropics (Rabah 2005), efficient harnessing of such energy, especially in drying of biological materials in sub-Saharan Africa, is still limited. This is due to the inadequate development of the exact science of harnessing and application of solar energy in the design of solar drying systems in this region, as most of the research has been carried out in the developed world (Kituu *et al*. 2010). In addition, the design of efficient and optimized solar energy-harnessing systems is of paramount importance in the utilization of solar energy in solar drying systems. Furthermore, Plantier *et al*. (2003) identified the cover, the collector plate and the moving fluid as the most important parts of solar energy-harnessing design. These are related to the transmission of solar energy into the collector and any reflective as well as radiative losses from the collector through the cover plate and the absorption and harnessing of energy from the collector plate to the drying air (Sukhatme 2003). The evaluation of the optimal values of the design input variables necessary for the improved performance of a dryer results in the optimization of the design of the dryer.

Remarkable research has been carried in the broad fields of solar energy harnessing and optimization of solar dryer design. Franke (1998) studied the modelling and optimal design of a central solar heating plant with heat storage in the ground using Modelica optimization tool. Similarly, Ajam *et al.* (2005) developed an exergetic optimization of solar air heaters and carried out a comparative performance evaluation using energy analysis. Smitabhindu *et al.* (2008) developed a mathematical model for optimal design of a solar-assisted drying system for drying bananas. In spite of the above research, there has been no research on the application of genetic algorithms (GAs) in the optimization of solar dryer designs.

GAs have been used in the optimization of various systems with a lot of success. For instance, Charron and Athienitis (2006) studied the use of GAs for a net-zero energy solar home design optimization tool. Although Thirugnanasambandam *et al.* (2010) undertook a review of solar thermal technologies, some of which apply GAs, they did not address the optimal design of solar dryers using GAs. In addition, Kalogirou (2004) studied the optimization of solar systems using artificial neural networks and GAs. The study involved the use of neural networks, whose dependability was based on the accuracy and consistency of the training data and the training process, and GAs. In addition, most of the research carried out in the broad field of optimization of solar tunnel dryers using GAs has been on the application of GAs in the optimization of excess capacity of renewable energy hybrid system (Razak *et al*. 2007) or on the comparison of GA and neural network approaches for the drying process (Erenturk and Erenturk 2007) as well as the optimization of the drying process of biological products using GAs (Khoshhal *et al*. 2010, Santana *et al*. 2010, Topuz and Hamzacebi 2010).

It is evident that although GAs have been applied in the optimization of several systems in several studies, such studies did not involve the use of GAs in the optimization of solar tunnel dryers. Based on the above observations, studies were carried out with the objectives of optimizing the design of solar tunnel dryers for drying of fish, in solar energy harnessing using GAs, and of developing the optimized dryers and evaluating their performance in the drying of fish.

2. Materials and methods

2.1. *Description of the experimental site*

This research was carried out at the Biomechanical and Environmental Engineering Department (BEED), Jomo Kenyatta University of Agriculture and Technology (JKUAT) in Juja township, 10 km West of Thika town and 45 km East of Nairobi, Kenya. The geoposition of the location is represented by 1.18 °S latitude, 37 °E longitude and an altitude of 1460 m, and the region experiences cold seasons between April and August and between October and December each year, with the rest of the period being dry hot seasons (Watako *et al*. 2001). The research was conducted between June and December 2009.

2.2. *The solar tunnel dryer*

The initial solar tunnel dryer system used in this study, exemplified schematically in Figure 1, had been developed at BEED in JKUAT. It consists of two main components: the air-heating chamber, also termed the tunnel chamber, and a drying section, termed the chimney-drying chamber. The air-heating chamber harnesses solar energy, converts it to heat energy and subsequently transfers it to the drying air in contact with a collector plate. Consequently, the temperature of the air is raised before it enters the drying chamber.

The tunnel chamber measures 2.4 m long, 1.2 m wide and 0.54 m high. It has a rectangular mild-steel collector plate, which is painted black for enhanced absorption and emission of solar energy, and a cover glass located above the collector plate. The cover glass acts as a green house to absorbed energy, which results in increased energy concentration in the tunnel chamber. The bottom side of this section is covered with aluminium-painted galvanized iron (GI) sheet to reflect energy incident on the surface. The rear side wall of the tunnel chamber is made of aluminium-coated GI sheet, while the front wall of the tunnel chamber has two sets of overlapping doors, through which thermocouples for data acquisition from the chamber are inserted. The inner walls of the doors are lined with aluminium-coated GI sheets, whereas the bottom and the side walls of the sheets are insulated with polystyrene sheets sandwiched between the inner and outer GI

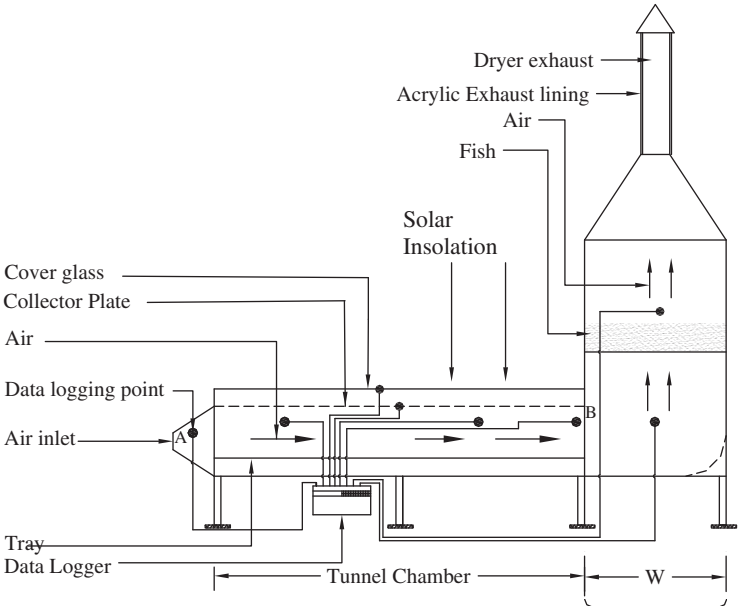

Figure 1. Solar tunnel dryer.

sheets to minimize energy losses. The chimney-drying chamber measures 1.2 m × 0.9 m × 0.7 m for the rectangular cross section and 1.2 m × 0.7 m at the bottom and 0.2 m × 0.2 m at the narrow end. It is made of GI sheets, with the inner walls coated with aluminium, while the outer walls are painted black. An exhaust system secured above the chimney-drying chamber is lined with acrylic material to enable solar heating of the exhaust air for increased air convection.

2.3. *Optimization simulation model*

In order to carry out the optimization process, it was necessary to express the physical system in a set of appropriate mathematical equations, as stated by Snyman (2005) and Charbonneau (2002). The analysis of the harnessed solar energy was carried out in terms of heating chamber air temperatures. This analysis assumed that there was no heat gain for or loss from the air-heating chamber, except heat losses, which can be evaluated using the overall heat loss coefficient. In addition, it assumed that the energy harnessed was under steady-state conditions and that the walls were adiabatic. The analysis approach similar to that carried out by Garg and Prakash (2000) and Sukhatme (2003) gave the temperature profile along the tunnel section of the dryer. Assuming that the inlet air temperature was equal to the ambient air temperature, the plenum chamber temperature, T_p, was given by Equation 1 (Kituu *et al*. 2010):

$$T_p = T_a + \left(\frac{I_c}{U_L}\right)\left(1 - \exp\left\{-\frac{A_c F' U_L}{\dot{m}_a C_p}\right\}\right). \quad (1)$$

The energy absorbed by the collector subjected to solar radiation was given by Equation 2 (Garg and Prakash 2000, Al–Ajlan *et al.* 2003, Sukhatme 2003). In order to evaluate the parameters I_b and I_d in Equation 2, it is necessary to evaluate the extra-terrestrial solar energy incident on a horizontal surface, H_o, as expressed in Equation 3 (Garg and Prakash 2000,

Al–Ajlan *et al.* 2003):

$$I_c = (I_b R_b + I_d R_d + (I_b + I_d) R_r A_b) \times (\tau\alpha)_e, \tag{2}$$

$$H_o = 10443.11(\cos\phi \cos\delta \sin\omega_s + \omega_s \sin\phi \sin\delta)\left(1 + 0.033\cos\left(\frac{360n}{365}\right)\right). \tag{3}$$

According to Jin *et al.* (2005), the global solar radiation, as a function of latitude, altitude and the ratio of possible to actual sunshine hours, can be expressed as in Equation 4. Based on Equation 4 and n, Equations 5 ($n \leq 120$), 6 ($120 < n < 310$) and 7 ($310 \leq n \leq 365$) were developed for determining I_g incident on a horizontal surface at the experimental site, with the parameters a_j and b_j represented by Equations 8 and 9 (Sukhatme 2003), respectively:

$$H_g = H_o \left\{ (0.0218 + 0.0033\phi + 0.0443 H_{alt}) + (0.9979 - 0.0092\phi - 0.0852 H_{asl}) \left(\frac{\bar{S}_p}{\bar{S}_a}\right) + (-0.5579 + 0.012\phi - 0.1 H_{asl}) \left(\frac{\bar{S}_p}{\bar{S}_a}\right)^2 \right\}, \tag{4}$$

$$I_g = 1.2545 \frac{\pi}{24} (H_g (a_j + b_j \cos\omega)) \left(\frac{(\cos\omega - \cos\omega_s)}{(\sin\omega_s - \frac{\pi\omega_s}{180}\cos\omega_s)}\right)\left(1 + 0.033\cos\left(\frac{360n}{365}\right)\right)^4 \cos^2\delta, \tag{5}$$

$$I_g = 1.0816 * \left(\frac{\pi}{24} H'_g (a_j + b_j \cos\omega)\right) \left(\frac{(\cos\omega - \cos\omega_s)}{(\sin\omega_s - \frac{\pi\omega_s}{180}\cos\omega_s)}\right) \times \left(1 + 0.033\cos\left(\frac{360n}{365}\right)\right)\cos^2\delta, \tag{6}$$

$$I_g = 1.4235 \left(\frac{\pi}{24} H'_g (a_j + b_j \cos\omega)\right) \left(\frac{(\cos\omega - \cos\omega_s)}{(\sin\omega_s - \frac{\pi\omega_s}{180}\cos\omega_s)}\right) \times \left(1 + 0.033\cos\left(\frac{360n}{365}\right)\right)^2 \cos^4\delta, \tag{7}$$

$$a_j = 0.409 + 0.5061 \sin(\omega_s - 60), \tag{8}$$

$$b_j = 0.6609 - 0.4767 \sin(\omega_s - 60). \tag{9}$$

The daily diffuse radiation (Equation 2) is influenced by k_t, given by Equation 10 (Al–Ajlan *et al.* 2003, Tarhan and Sari 2005). In addition, based on k_t and ω_s, H_d was evaluated from Equations 11 ($\omega_s > 81.4^\circ$ and $k_t \leq 0.8$) and 12 ($\omega_s \leq 81.4^\circ$ and $0.3 \leq k_t < 0.8$) (Garg and Prakash 2000). Furthermore, based on Equations 11 and 12, the hourly diffuse solar radiation, I_d, was given by Equation 13 (Al–Ajlan *et al.* 2003). Furthermore, the hourly beam radiation, I_b, incident on a horizontal surface was computed from Equation 14 (Garg and Prakash 2000, Al–Ajlan *et al.* 2003):

$$k_t = \frac{H_g}{H_o}, \tag{10}$$

$$H_d = H_g(1.311 - 3.022 k_t + 3.427 k_t^2 - 1.821 k_t^3), \tag{11}$$

$$H_d = H_g(1.311 - 3.560 k_t + 4.189 k_t^2 - 2.137 k_t^3), \tag{12}$$

$$I_d = \left(\frac{\pi H_d}{24}\right)\left(\frac{\cos\omega - \cos\omega_s}{(\sin\omega_s - (\pi\omega_s\cos\omega_s)/180)}\right), \tag{13}$$

$$I_b = I_g - I_d. \tag{14}$$

The parameters I_b and I_d are important input variables in evaluating I_c (Equation 2), which forms an important input variable in the determination of the plenum chamber temperature (Equation 1).

2.4. *Data acquisition*

2.4.1. *Optimization with GAs*

Prior to the optimization of solar energy harnessing by the solar tunnel dryer, the harnessed energy, exemplified by T_p (see Equation (1)), was simulated using Visual Basic 6 (Microsoft Visual Basic 6.0™) computer programming language. A free-source GA named Goal was downloaded from the internet. The GA, developed by Angela Martin of the University of Valladolid (Spain), is capable of solving complex problems formulated in real or binary coding with several variables and constraints and with complex objective functions. Coded in Visual Basic Script (Microsoft Visual Basic Script 2010™), the algorithm facilitates the formulation of optimization problems through a graphic user interphase (Figure 2) where variables are declared and entered into the algorithm. The simulation model for the harnessed energy was coded in Visual Basic Script. Thereafter, the variables were declared before execution of the algorithm. When executed, the algorithm undergoes the iterative processes of selection, encoding, crossover, mutation, decoding, and evaluation of fitness and replacement of the parents with off-springs. The algorithm loops the process until it meets the termination criteria as set in Equation 15. The GA allows the use of default values of its parameters or the modified values as shown in Table 1. The modification of the input variables alters the convergence of the algorithm, and it is desirable to improve the convergence, although this could introduce a longer convergence period. The execution of the GA

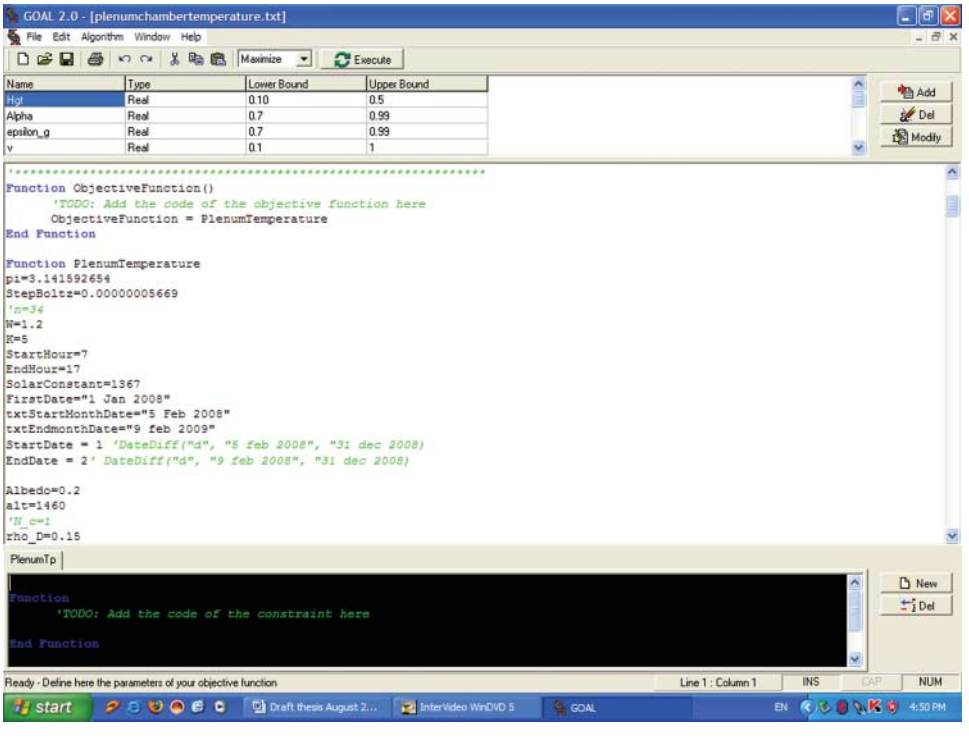

Figure 2. The graphic user interphase for Goal GA.

Table 1. GA parameters.

Parameter	Default value	Value used
Population	30	60
Generations	80	100
Reproduction cross-over points	2	3
Reproduction probability	0.95	0.99
Selection type	Elitism tournament	Elitism tournament
Mutation probability	0.005	0.001
Reproduction probability	0.80	0.99
Selection probability	0.95	0.99
Elitism-preserved individuals	2	2
Population refresh period (generations)	40	60
% population refreshed	10	10

followed the flow process shown in Figure 3:

$$\begin{aligned} &\text{maximize} \quad T_{\mathrm{p}} = T_{\mathrm{a}} + \left(\frac{I_{\mathrm{c}}}{U_{\mathrm{L}}}\right)\left(1 - \exp\left\{-\frac{A_{\mathrm{c}}F'U_{\mathrm{L}}}{\dot{m}_{\mathrm{a}}C_{\mathrm{p}}}\right\}\right) \\ &\text{subject to} \quad \{60 \le T_{\mathrm{p}}, 0 \le A_{\mathrm{c}} \le 15, 0 \le b_{\mathrm{d}} \le 1.1, 0 \le \mathrm{V} \le 15\}. \end{aligned} \tag{15}$$

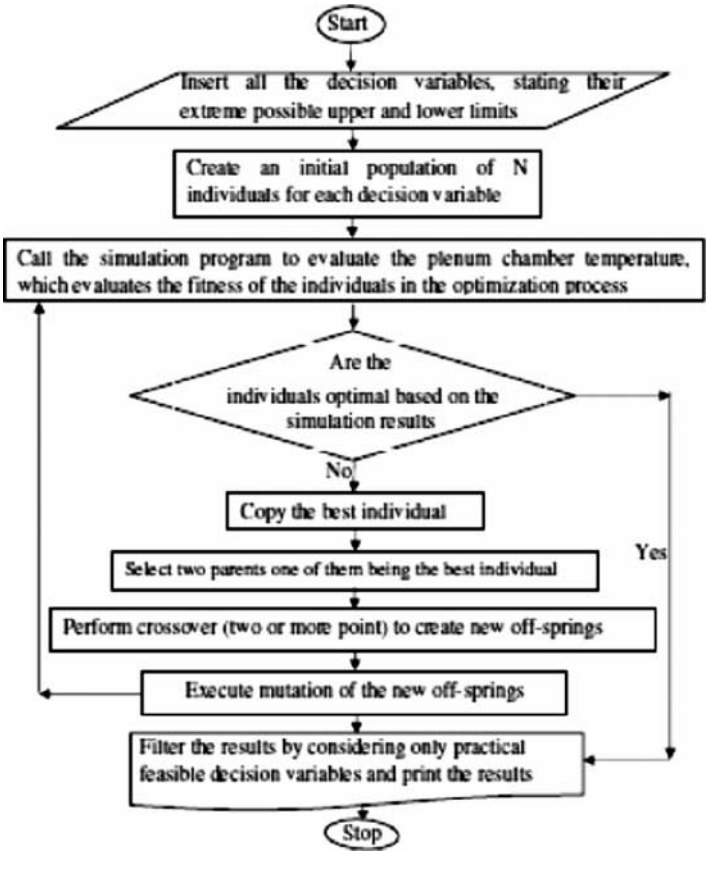

Figure 3. A flow chart for optimizing solar tunnel dryer using GA.

2.4.2. *Construction of the optimized solar tunnel dryer*

Based on the optimization results obtained above, the solar tunnel dryer used in the validation of the simulation models (Figure 1) required modifications. The modifications made on it included a reduction of the depth of the air-heating chamber and the drying chamber from 0.54 to 0.11 m and 0.7 to 0.27 m, respectively. The other parameters (viz. heating-chamber and drying-chamber lengths and widths, bottom-plate and side-wall material thickness and thickness of insulation) remained as in the existing dryer (Figure 1). A schematic diagram of the heating and drying chambers of the optimized dryer is presented in Figure 4.

2.4.3. *Experimental set-up and data acquisition*

Despite the optimized dryer being different from the existing dryer, the relative positions of the various points used to measure the temperatures generated in either the optimized or the existing solar tunnel dryer were as those shown in Figure 1. The ambient and plenum chamber temperatures were measured at points A and B (Figure 1), respectively. The measurements were carried out using thermocouples, which logged the temperatures to an automatic electronic data logger (Thermodac Eto Denki E, Shimadzu, Japan). In addition, ambient humidity and plenum chamber air humidity were measured using thermo–hygro sensor units. Each of the thermo–hygro sensor units used has three components: a sensor which is usually placed at the point of humidity measurement, a display unit and a cable which relays data from the sensor to the display unit.

In order to evaluate the performance of the optimized solar tunnel dryer, it was necessary to collect and compare data under four different treatments. Treatments 1 and 2 corresponded to the drying process in the existing solar tunnel dryer and the optimized solar tunnel dryer, respectively. In addition, Treatments 3 and 4 corresponded to open sun drying carried out simultaneously with the drying in the existing and the optimized solar tunnel dryers, respectively. Data under Treatments 1 and 3 were initially acquired simultaneously for three consecutive days. Thereafter, the dryer was modified within 1 day in conformity with the optimized design variables obtained with the Goal GA and then evaluated under Treatments 2 and 4 immediately for another three consecutive days. The reason for not evaluating the data for Treatments 1 and 2 simultaneously was the high cost involved in the construction of the two drying systems. The data acquired included the plenum chamber temperature, the ambient temperature and the ambient and plenum chamber humidity.

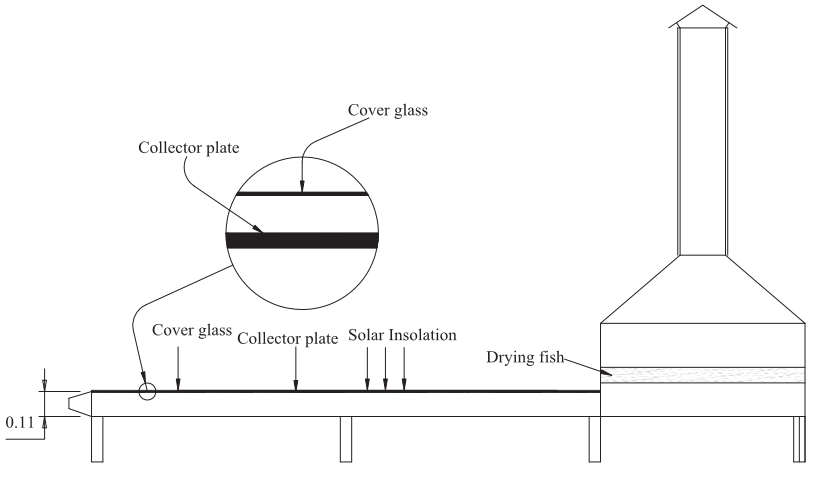

Figure 4. Schematic diagram of the optimized solar tunnel dryer.

2.5. *Data analysis*

To evaluate and compare the performance of the optimized and existing solar tunnel dryers, air ambient and plenum chamber temperatures and humidity values were obtained for both dryers. The data obtained were analysed in MS Excel 2007 (MS Excel 2007™), using graphical methods, regression analysis, analysis of variance (ANOVA) and Student's *t*-test.

3. Results and discussions

3.1. *Energy harnessing and optimization using GAs*

The design variables which yielded plenum chamber temperatures close to the desired value of 60°C are presented in Table 2, from which the highlighted set of variables was selected as the most optimal design variables. Based on these data, an optimized solar tunnel dryer, schematically represented in Figure 4, was constructed and its performance in energy harnessing was evaluated against that of the existing dryer.

Figure 5 presents the mean of 5-day plenum chamber and ambient air temperatures for optimized and the existing solar tunnel dryer systems, which were acquired under Treatments 1, 2, 3 and 4 (see Section 2.4.3). In addition, Figure 5 shows that the plenum chamber temperatures for the optimized solar tunnel dryer were higher than those for the existing dryer. This fact is further supported by the ratios of optimized dryer plenum chamber temperatures to those of the existing dryer (Table 3), which show that the ratio ranged from 0.91 to 2.13, with a mean of 1.32. Furthermore, the ratio was always higher than 1, except at 6.00 p.m., when it fell to 0.91. Additionally, the ratio of plenum chamber temperatures to ambient temperatures for optimized and existing solar tunnel dryers varied from 0.63 to 1.47 and 0.81 to 1.91, respectively. Furthermore, the percentage increase in

Table 2. Optimal design variables generated by Goal GA.

L (m)	b_d (m)	A (m^2)	w (m)	V (m^3)	v (m/s)	β (°)	H	T_p (°C)
2.45	0.11	0.2695	1.15	0.30992	0.05	0.89	1.31	59.6
2.45	0.11	0.2695	1.16	0.31262	0.05	0.97	1.31	59.2
2.40	0.10	0.2400	1.24	0.29760	0.05	0.58	1.40	56.8
2.43	0.11	0.2673	1.16	0.31006	0.05	0.59	1.44	58.8
2.45	0.11	0.2695	1.17	0.31531	0.05	0.42	1.31	57.9
2.45	0.10	0.2450	1.16	0.28420	0.05	0.71	1.31	58.2
2.35	0.11	0.2585	1.22	0.31537	0.05	0.58	1.35	59.6
(2.44)	(0.11)	(0.2684)	(1.22)	(0.32744)	(0.05)	(0.07)	(1.31)	(60.0)
2.40	0.10	0.2400	1.17	0.28080	0.05	0.87	1.37	56.5
2.43	0.10	0.2430	1.20	0.29160	0.05	0.42	1.31	57.2
2.45	0.11	0.2695	1.16	0.31262	0.05	0.90	1.31	55.3
2.44	0.10	0.2440	1.18	0.28792	0.06	0.92	1.30	57.3
2.43	0.11	0.2673	1.16	0.31006	0.05	0.91	1.32	57.6
2.35	0.10	0.2350	1.20	0.28200	0.05	0.95	1.34	58.7
2.42	0.11	0.2662	1.15	0.30613	0.05	0.12	1.42	58.9
2.45	0.11	0.2695	1.15	0.30992	0.05	0.99	1.34	59.4
2.42	0.10	0.2420	1.21	0.29282	0.06	1.00	1.33	57.6
2.45	0.10	0.2450	1.18	0.28910	0.05	0.80	1.32	57.2
2.38	0.10	0.2380	1.18	0.28084	0.05	0.98	1.44	55.8
2.41	0.10	0.2410	1.16	0.27956	0.06	0.88	1.30	55.8
2.41	0.10	0.2410	1.23	0.29643	0.05	0.79	1.46	57.6
2.42	0.10	0.2420	1.15	0.27830	0.05	0.61	1.55	58.2

Notes: The parameters given in the parentheses represent the optimal values. L, collector plate length; b_d, air-heating chamber depth; A, collector plate surface area; w, collector plate width; V, air-heating chamber volume; v, air flow velocity; β, tilt angle; η, cover glass refractive index; T_p, plenum chamber temperature.

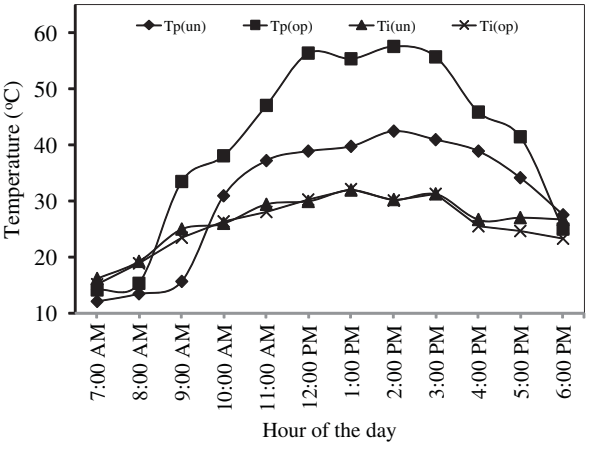

Figure 5. Daily ambient and plenum chamber temperatures.

plenum chamber temperature varied between 18 and 113%, except at 6.00 p.m., when the increase was −9%. The above observations show that the optimized solar tunnel dryer performed better in solar energy harnessing than the existing dryer.

In order to establish the existence of a difference between the drying temperatures under Treatments 1, 2, 3 and 4, a two-factor ANOVA was performed. The results of the analysis confirmed the existence of a highly significant difference between the temperatures under the four treatments ($F = 16.37, F_{\text{crit},0.95} = 2.89, F_{\text{crit},0.99} = 2.89$). Similarly, a two-way Student's t-test showed the existence of a significant difference between the temperatures under Treatments 1 and 2 ($t_{\text{stat}} = 9.62$; $t_{\text{crit},5\%} = 2.2$, $t_{\text{crit},1\%} = 3.11$). However, Student's t-test did not show the existence of any significant difference between the temperatures under Treatments 3 and 4 ($t_{\text{stat}} = 0.005$; $t_{\text{crit},5\%} = 2.2$, $t_{\text{crit},1\%} = 3.11$). The above results show that the optimized solar tunnel dryer generated higher temperatures than the non-optimized solar tunnel dryer, despite the ambient conditions not being different. In addition, these results show that there was a highly significant difference

Table 3. Post-optimization and pre-optimization open sun and plenum chamber temperatures (°C) and temperature ratios.

	Inlet temperature		Plenum temperature		Temperature ratios			
Hour	Optimized	Non-optimized	Optimized	Non-optimized	Optimized to inlet	Non-optimized to inlet	Optimized to non-optimized	$\%\Delta T_p^a$
7.00 a.m.	15.2	16.2	14.15	12.12	0.93	0.75	1.17	17
8.00 a.m.	18.9	19.3	15.3	13.4	0.81	0.7	1.14	14
9.00 a.m.	23.5	24.9	33.5	15.7	1.43	0.63	2.13	113
10.00 a.m.	26.3	25.9	38	31	1.44	1.2	1.23	23
11.00 a.m.	28	29.4	47	37.3	1.68	1.27	1.26	26
12.00 p.m.	30.2	30	56.35	38.9	1.87	1.3	1.45	45
1.00 p.m.	32.1	32	55.43	39.8	1.73	1.24	1.39	39
2.00 p.m.	30.1	30.2	57.6	42.5	1.91	1.41	1.36	36
3.00 p.m.	31.3	31.2	55.8	41	1.78	1.31	1.36	36
4.00 p.m.	25.5	26.6	45.98	39	1.8	1.47	1.18	18
5.00 p.m.	24.7	27	41.45	34.2	1.68	1.27	1.21	21
6.00 p.m.	23.2	26.6	24.9	27.5	1.07	1.03	0.91	−9
Mean					1.51	1.13	1.32	

[a] ΔT_p is the change in plenum chamber temperature (°C).

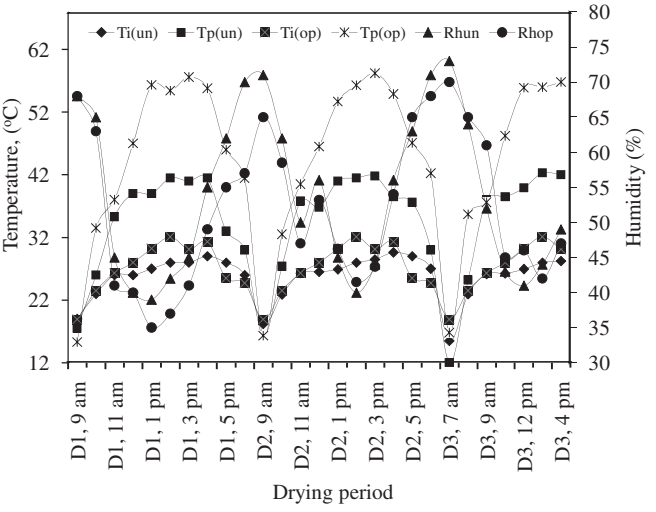

Figure 6. Ambient and plenum chamber air temperatures and plenum relative humidites during the evaluation of optimized solar tunnel dryer. Rhun, unoptimized solar tunnel dryer relative humidity; Rhop, optimized solar tunnel dryer relative humidity.

between the temperatures developed by the optimized solar tunnel dryer and those developed by the non-optimized solar tunnel dryer. Furthermore, the results demonstrate the ability of using the Goal GA in the optimization of a solar tunnel dryer.

Based on the regression analysis, a strong linear correlation was established between ambient and plenum chamber temperatures for the optimized solar tunnel dryers (coefficients of determination, $R^2 = 0.961$) and the existing dryer ($R^2 = 0.816$). However, the R^2 values show that the correlation between the plenum chamber and ambient temperatures was stronger for the optimized solar tunnel dryer than for the existing solar tunnel dryer. The above observations imply that the optimized solar tunnel dryer was more sensitive to variations in ambient air temperatures. Consequently, any changes in air temperatures would result in variations in plenum chamber temperatures. This further demonstrates the improvement in the ability of the optimized solar tunnel dryer to harness energy in comparison with the existing dryer.

The relative humidity and air temperatures in the solar tunnel dryers at the time of drying under the four treatments are presented in Figure 6. The figure shows that the humidity of air varied conversely with the air temperatures. The relative humidity was much lower in the optimized solar tunnel dryer than in the existing solar tunnel dryer. This is an indication of the superiority of the optimized solar tunnel dryer to reduce the relative humidity of air and subsequently increase the potential of the air to absorb moisture.

4. Conclusions and recommendations

An optimized solar tunnel dryer was bred artificially using a simulation model and Goal GA. The optimization process resulted in the reduction of the air-heating chamber depth by a factor of 4.91. In addition, validation results show that higher plenum chamber temperatures were obtained for the optimized dryer (2.4 m long, 1.20 m wide and 0.11 m) than for the non-optimized one (2.24 m long, 1.20 m wide and 0.54 m), and these were found to be significantly different. It was also noted that the fish drying process took 15 h for the drying to reach equilibrium moisture content of 0.12 kg/kg, dry basis for the optimized dryer when compared with 22 h for the

non-optimized one. In addition, Student's t-test results established the existence of a significant difference between the moisture ratios for fish dried in the optimized and non-optimized solar tunnel dryers ($t_{\text{stat}} = -6.828$; $t_{\text{crit},5\%} = 2.048$, $t_{\text{crit},1\%} = 2.763$). The above results show that there was a highly significant difference between the temperatures developed by the optimized solar tunnel dryer and those developed by the existing solar tunnel dryer, despite the ambient conditions not being different. Finally, these observations imply that the optimized solar tunnel dryer is superior to the existing solar tunnel dryer in solar energy harnessing and demonstrate the strength of application of GAs in breeding better solar tunnel dryers.

Acknowledgements

The authors acknowledge the financial support extended to this research by *VicRes*, an SAREC-sponsored L. Victoria Research Programme, and the support in terms of research facilities from Jomo Kenyatta University of Agriculture and Technology. The contribution by Angela Martin of the University of Valladolid (Spain) in availing a free-source Goal genetic algorithm (Angela Martin©), downloadable at www.oocities.com/geneticoptimisation, which was used in this study, is highly appreciated.

References

Ajam, H., Farahat, S., and Sarhaddi, F., 2005. Exergetic optimization of solar air heaters and comparison with energy analysis. *International Journal of Thermodynamics*, 8 (4), 183–190.

Al–Ajlan, S.A., Al–Faris, H., and Khonkar, H., 2003. A simulation modeling for optimization of flat plate collector design in Riyadh, Saudi Arabia. *Renewable Energy*, 28, 1325–1339.

Charbonneau, P., 2002. *An introduction to genetic algorithms for numerical optimization*. Boulder-Colorado: National Center for Atmospheric Research (NCAR), High Altitude Observatory National Center for Atmospheric Research, Technical Note, March 2002.

Charron, R. and Athienitis, A., 2006. The use of genetic algorithms for a net-zero energy solar home design optimisation tool. *In: The proceedings of the 23rd conference. Passive and low energy architecture* (*PLEA2006*), 6–8 September 2000. Geneva, Switzerland. Available from http://canmetenergy-canmetenergy.nrcan-nrcan.gc.ca/fichier.php/codectec/en/2006-161/2006-161e.pdf

Erenturk, S. and Erenturk, K., 2007. Comparison of genetic algorithm and neural network approaches for the drying process of carrot. *Journal of Food Engineering*, 78, 905–912.

Franke, R., 1998. Modelling and optimal design of a central solar heating plant with heat storage in the ground using Modelica. *In: The proceedings of the Eurosim '98 simulation congress*, April 1998, Espoo, Finland. Available from http://www.modelica.org/papers/FrankeEurosim98.ps

Garg, H.P. and Prakash, J., 2000. *Solar energy: fundamentals and applications*. 1st revised ed. New Delhi, India: Tata McGraw Hill Publishers.

Jin, Z., Yezheng, W., and Gang, Y., 2005. General formula for estimation of monthly average daily global solar radiation in China. *Energy and Conservation Management*, 46, 257–268.

Kalogirou, S.A., 2004. Optimization of solar systems using artificial neural-networks and genetic algorithms. *Applied Energy*, 77, 383–405.

Kituu, G.M., *et al.*, 2010. Simulation model for solar energy harnessing by the solar tunnel dryer. *Agricultural Engineering International: The CIGR Journal*, 12 (1), 91–98.

Plantier, C., Fraisse, G., and Achard, G., 2003. Development and experimental validation of a detailed flat-plate solar collector model. *In: ISES solar world congress*, 14–19 June 2003. Göthenborg, Sweden. Available from http://enr.cstb.fr/file/rub17_doc12_2.pdf

Rabah, K.V.O., 2005. Integrated solar energy systems for rural electrification in Kenya. *Renewable Energy*, 30, 23–42.

Razak, J.A., Sopian, K., and Ali, Y., 2007. Optimization of renewable energy hybrid system by minimizing excess capacity. *International Journal of Energy*, 1 (3), 76–81.

Santana, J.C.C., *et al*., 2010. Optimization of corn malt drying by use of a genetic algorithm. *Drying Technology*, 28 (11), 1236–1244.

Smitabhindu, R., Janjai, S., and Chankong, V., 2008. Optimization of a solar-assisted drying system for drying bananas. *Renewable Energy*, 33 (7), 1523–1531.

Snyman, J.A., 2004. *Practical mathematical optimization: an introduction to basic optimization theory and classical and new gradient-based algorithms*. Dordrecht: Kluwer.

Sukhatme, P.K., 2003. *Solar energy: principles of thermal collection and storage*. 2nd ed. New Delhi, India: Tata McGraw-Hill Publishing.

Tarhan, S. and Sari, A., 2005. Model selection for global and diffuse radiation over the Central Black Sea (CBS) region of Turkey. *Energy Conservation and Management*, 46, 605–613.

Thirugnanasambandam, M., Iniyan, S., and Goic, R., 2010. A review of solar thermal technologies. *Renewable and Sustainable Energy Reviews*, 14, 312–322.

Topuz, A. and Hamzacebi, C., 2010. Moisture ratio prediction in drying process of agricultural products: a new correlation model. *Applied Engineering in Agriculture*, 26 (6), 1005–1011.

Watako A.O., *et al*., 2001. The effect of rootstock on budtake and budgrowth vigour of rose(*Rosa* spp.) cultivar (First Red). *Journal of Agriculture, Science and Technology*, 1, 57–67.